Digest Journal of Nanomaterials and Biostructures Vol. 19, No. 4, October-December 2024, p. 1693-1699

Sensing capability of molten salt synthesize (K, Na) NbO_3 ceramic powder

D. S. Chakram [a], U. Godavarti [b], C. Kavitha [a], M. Dasari [a,*]
[a] *Department of Physics, GITAM School of Science, GITAM (Deemed to Be University), Visakhapatnam-45, India*
[b] *Department of Physics, CMR technical campus, Hyderabad, Telangana, India*

At room temperature, $K_{0.5}Na_{0.5}NbO_3$ ceramic particles were tested for sensing. This study synthesized $K_{0.5}Na_{0.5}NbO_3$ particles using molten salts. X-ray diffraction and scanning electron microscopy were employed to understand the material. The gas-sensing properties of a novel material family are greatly improved. Sodium potassium niobate granules detect ammonia at room temperature. This material offers excellent temporal sensitivity and a quick response. The sample has oxygen shortages, according to Photoelectron X-ray spectroscopic investigations.

(Received August 12, 2024; Accepted November 4, 2024)

Keywords: Lead-free ceramics, Inorganic materials, Molten salt synthesis, Gas sensing, Photoelectron X-ray spectroscopy

1. Introduction

Lead zirconium titanates (Pb, Zr) TiO_3 (PZT) are widely used due to their outstanding piezoelectric capabilities despite environmental degradation issues. Materials like piezoelectrics can transform mechanical and electrical energy. Sensors, actuators, and transducers are increasingly made from smart materials [1-6]. Lead in piezo-electrics is restricted by environmental rules due to its dangers to humans and the environment.

Lead oxide's toxicity during firing pollutes the environment and harms humans [7-9]. Lead-free ceramics have inferior piezoelectric properties to PZT ceramics, but substantial effort is being put into synthesizing them with enhanced characteristics. Recently, lead-free piezo ceramics have garnered interest as a piezoelectric material with significant benefits in lead-free surroundings. Potassium sodium niobate oxides, bismuth layer structured oxides, and bismuth sodium titanates are being investigated as lead-free piezoelectric materials. $K_{0.5}Na_{0.5}NbO_3$ is denoted as KNN ceramics' vulnerability to non-stoichiometry, the complexity of densification, and the need for specialist source powder treatment, which are its main drawbacks. Alkaline carbonates are more water-soluble. Water processing can create stoichiometric errors during ceramic processing, deteriorating sintered samples. The strong alkalinity of ceramic powders reacts quickly with atmospheric humidity, causing deliquescence. The low melting point (1058°C) of $KNbO_3$ hinders sinterability in the KNN system. Pure KNN ceramic loses phase stability at 1140°C, as per $KNbO_3$ and $NaNbO_3$ phase diagrams. These materials' alkaline metal components evaporated easily at high temperatures. Hot-press, hot-isostatic press, hydrothermal, sol-gel, spark-plasma sintering, and molten salt synthesis of KNN-based ceramics have been studied extensively. A high Curie point Tc, piezoelectric longitudinal action, and large planar coupling coefficient were found in hot-pressed KNN ceramics. Spark-plasma sintering allows lead-free materials for various uses. Normal ceramic sintering is difficult for thick ceramics, so KNN ceramics sintered by hot-press and hot-isostatic presses are unsuitable for industrial applications. Spark-plasma sintering isn't usually industrially viable. Industrial mass production requires conventional sintering. Several studies have examined KNN-based ceramics using solid-state sintering. [10]. $K_{1-x}Na_xNbO_3$ at x=1/2, with its Morphotropic Phase Boundary (MPB) between orthogonal and tetragonal phases (O-T phase), caught the researcher's interest and inspired them to study lead-free piezoceramics [1, 9–15].

* Corresponding author: madhavaprasaddasari@gmail.com

https://doi.org/10.15251/DJNB.2024.194.1693

Many research methods have improved KNN's physical properties. The efficient molten salt synthesis (MSS) of $K_{0.5}Na_{0.5}NbO_3$ powders in this study may replace mixed oxide. Many ceramic powders are produced fast using molten salt synthesis. Complicated systems with molten salt are easy to prepare by using MSS. Components with high diffusivity may reduce reaction time and temperature. MSS controls particle shape. Hence, tape casting makes grain-oriented ceramic [16,17].

MSS is a simple and modest strategy to generate single-crystal particles in a low melting point flux. By controlling particle shape, molten salt synthesis at low calcination temperatures forms the appropriate phase and produces grain-oriented ceramics.

Gas sensing has been researched alongside KNN-based ceramics. Environmental contamination rises with urbanization. Thus, novel sensing materials are needed to detect poisonous and dangerous atmospheric chemicals. Over the past decade, researchers have examined different sensing materials [18-21]. This may be one of the few articles on lead-free KNN, which are superior sensing materials [22].

2. Material and methods

Using molten salt synthesis, $K_{0.5}Na_{0.5}NbO_3$ lead-free ceramics were created. The stoichiometric ratio weighs K_2CO_3 (98%), Na_2CO_3 (99%), and Nb_2O_5 (99.9%). The inorganic salts NaCl (99.5%) and KCl (99.5%) were mixed equally i.e., 1:1 ratio. A mortar and pestle were used to hand-grind precursors and salts 1:1 for one hour. Grinding proceeded for 5–6 hours in acetone. The mixes were calcined at 750°C for 2 hours in alumina crucibles. Ultrasonication was used to wash the particles in deionized water. The wet powders are then oven-dried to remove all moisture and made 10mm pallets under seven tones of pressure using a 5% PVA binder. Sintered at 1050°C for 3 hrs. Bruker D8 discovery performed XRD. The phase was identified using XRD investigation from 2θ = 10 to 80 degrees. SEM (Quanta 200, FEI) equipped with EDS (Genesis) was used for electron microscopy. Keithley electrometer (6517B, USA) is used for the sensing application,Which is a cylindrical flask, gas-sensing chamber, and computer connected to a sensitive electrometer.

3. Results and discussion

3.1. XRD analysis

All calcined samples are checked for phase and purity. We found an additional phase in $K_{0.5}Na_{0.5}NbO_3$.

Previous results [23] indicate a peak at 2θ=32° without splitting in $KNbO_3$, but $NaNbO_3$ and $K_{0.5}Na_{0.5}NbO_3$ show peak splitting [23, 24]. In this study, KNN materials exhibit typical peaks around 2θ=46°, indicating an orthorhombic phase.

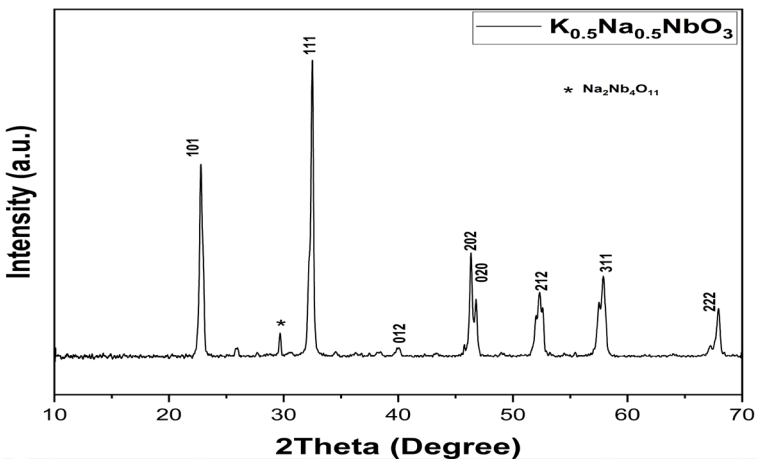

Fig. 1. XRD pattern of $K_{0.5}Na_{0.5}NbO_3$ ceramics.

Figure 1. shows another phase equivalent to $Na_2Nb_4O_{11}$ was observed, which shows a perovskite nature that is similar to $KNbO_3$ orthorhombic perovskite (JCPDS 71-2171) in the $K_{0.5}Na_{0.5}NbO_3$ sample. The above XRD plot and data were collected from earlier research [18].

3.2. Rietveld refinement

Rietveld refinements of the XRD patterns are conducted for all the samples and are shown in Figure. 2. Obtained parameters tabulated from Rietveld refinement and compared with the standard orthorhombic lattice parameters.

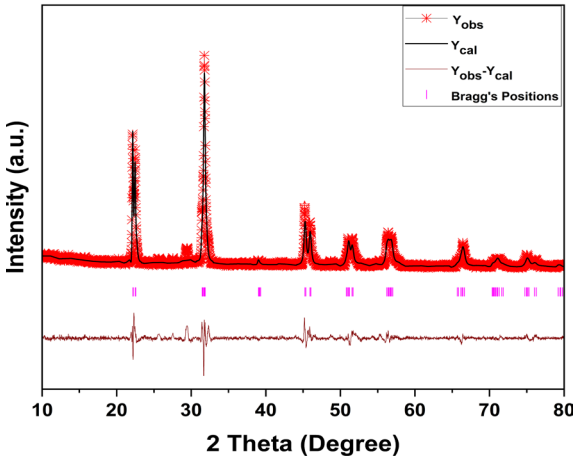

Fig. 2. Rietveld refinement of $K_{0.5}Na_{0.5}NbO_3$.

Table 1. Parameters were obtained from Rietveld refinement of $K_{0.5}Na_{0.5}NbO_3$.

Sample	Lattice parameters	Volume	Chi^2	GOF
$K_{0.5}Na_{0.5}NbO_3$	a=3.9495, b=5.6465, c=5.6839. α= β= γ=90°	126.70	3.01	1.7

3.3. Electron microscopic studies

$K_{0.5}Na_{0.5}NbO_3$ microstructure was studied using scanning electron microscopy with energy dispersive analysis. Image J program yields an average particle size of 0.67 µm. Used distributive curves to explain this [18].

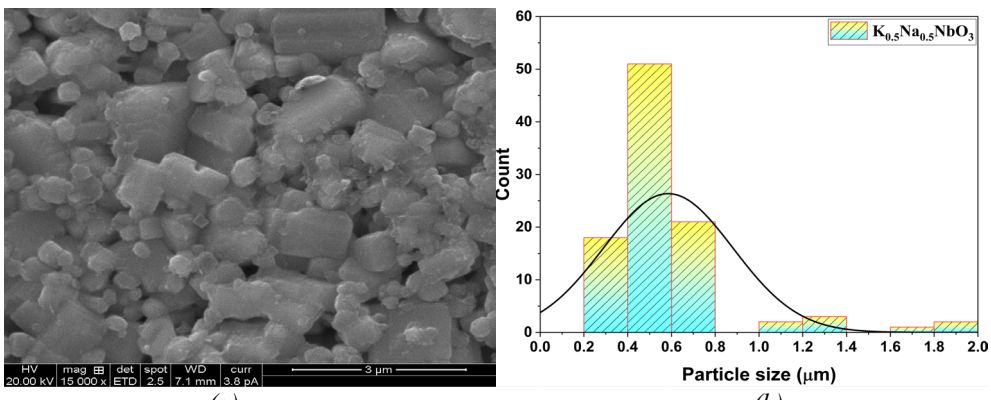

(a) *(b)*

Fig. 3. (a). SEM image of $K_{0.5}Na_{0.5}NbO_3$ ceramic and (b) particle size distributive curves of

$K_{0.5}Na_{0.5}NbO_3$ ceramic.

Figure 3(a) shows a $K_{0.5}Na_{0.5}NbO_3$ SEM image on a 3 µm scale at 15000 magnification. Figure 3 (b) shows particle size distributive curves. The above SEM Image and data were collected from earlier research [18].

3.4. Gas sensing studies

Novel gas sensors have been developed for environmental monitoring and automotive, medical, and indoor air quality applications throughout the past few decades [25]. Since ammonia (NH_3) is one of the most widely manufactured and utilized chemicals, gas sensors are interested in it.

Lower ammonia gas concentrations react to $K_{0.5}Na_{0.5}NbO_3$, and the sensor system includes a cylindrical flask, gas-sensing chamber, computer, and sensitive Keithley electrometer (6517B, USA). Chambers enclose samples. Gas enters the chamber through an input port and leaves via an output port connected to an air pump. Ammonia is injected into the chamber from the input port with a syringe. The output port should now be closed. After measuring the sample's resistance to ammonia gas (air and ammonia), open the exit port to let the gas out and measure the gas response (percentage) and recovery time.

The sensor response is the ratio of the sample's change in gas (Rg) and air (Ra) resistance to its air resistance. The following relation determines gas sensitivity (S) [21,25].

$$S = \frac{(\mathrm{Ra} - \mathrm{Rg})}{\mathrm{Ra}} \times 100$$

The response curves of $K_{0.5}Na_{0.5}NbO_3$, shown in the below Fig. 6.

Oxides sense gas by structural sensitization and resistance changes produced by target gas adsorption and desorption. Stability is crucial to sensors. Foreign atoms have also been shown to improve sensor element stability in $K_{0.5}Na_{0.5}NbO_3$. The new study's gas-detecting method: Filling the oxygen-vacancy defect with ammonia heals the carrier trap [25].

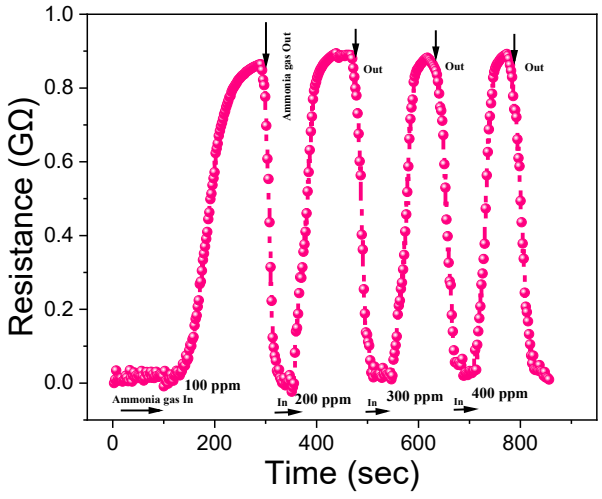

Fig. 4. Ammonia gas sensitivity response with respect to time.

From Figure. 4, KNN sample sensitivity peaked at 86% at 100 ppm gas. In $K_{0.5}Na_{0.5}NbO_3$ samples, 100, 200, 300, and 400 ppm gas concentrations boosted the reaction, time-dependent sensitivity response (%) in $K_{0.5}Na_{0.5}NbO_3$ due to oxygen vacancies.

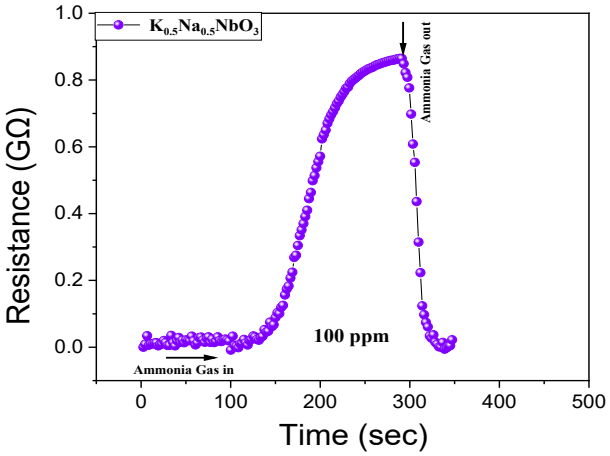

Fig. 5. Ammonia gas sensitivity and recovery time at 100ppm.

Figure 5 represents that, at 100 ppm, the pure $K_{0.5}Na_{0.5}NbO_3$ reaction at 100 ppm lasted 137-293 seconds. Reaction time is the time it takes to reach 90% of the maximum sensing response when the gas is turned on, and recovery time is the time it takes to return to 10% upon turning off. Response and recovery took 102 and 172 seconds, respectively. Due to fast O^- or O_2^- oxidation, diffusion speeds the sensor response mechanism of ammonia gas sensing [26].

$$O_{2(atmosphere)} + e^-_{(KNN\ surface)} \rightarrow O^-_{2(KNN\ surface)}$$

$$4NH_3 + 3O^-_{2(ads)} \rightarrow 2N_2 + 6H_2O + 3e^-$$

The fast response time shows that $K_{0.5}Na_{0.5}NbO_3$ is acceptable for sensing, and longer recovery time may be due to ammonia desorption at higher concentrations [27].

3.5. XPS analysis for oxygen deficiency

Samples were tested for oxygen deprivation using XPS. The deconvolution of the O_{1s} peak revealed three internal peaks at 529, 531, and 533 eV, labeled O^{2-}, O-, and O_2^-. The low energy peak around 529 eV represents oxygen at perovskite lattice or surface O^{2-} [28], the second peak at 531 eV represents oxygen at dissociative or deficiency regions, and the third peak at high binding energy around 533 eV represents molecular type [26,27].

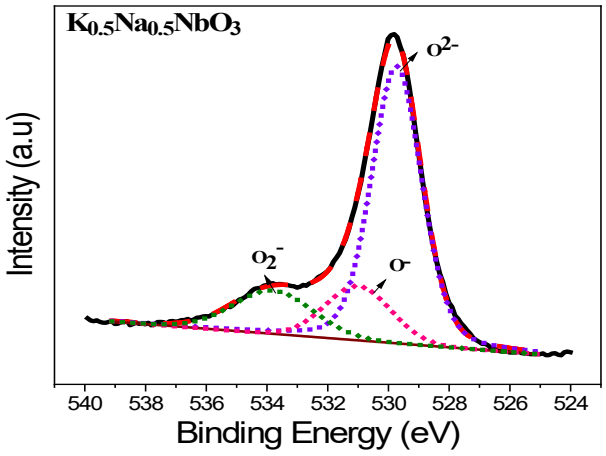

Fig. 6. XPS spectra of $O1_s$ peak for $K_{0.5}Na_{0.5}NbO_3$

Figure 6 shows that $K_{0.5}Na_{0.5}NbO_3$ has 31.34% oxygen shortage and adsorbate regions. These two regions are attributed to sensing [28]. Sodium potassium niobate sensors detect ammonia well.

4. Conclusions

$K_{0.5}Na_{0.5}NbO_3$ was prepared in molten salt synthesis. In 2 hours at 750°C calcination temperature, the sample revealed the orthorhombic phase with the Amm2 Space group. The time-sensitive behavior of ammonia gas has been studied. Due to oxygen shortage, $K_{0.5}Na_{0.5}NbO_3$ senses all gas concentrations quickly. X-ray Photoelectron Spectroscopy showed more oxygen deficits. $K_{0.5}Na_{0.5}NbO_3$ has a substantial ammonia gas-detecting response. They can be used to detect ammonia due to their exceptional sensing properties.

Acknowledgements

The authors would like to thank UGC–DAE–Consortium for scientific research (University Grants Commission–Department of Atomic Energy–Consortium for Scientific research), Indore for sanction of research project and financial support. All authors are grateful to Dr. Varimalla Raghavendra Reddy, Scientist H, for his unwavering support, mentoring, and guidance throughout the project. This research works on perovskite-based lead-free ceramics was supported by the UGC–DAE–Consortium for Scientific Research (University Grants Commission–Department of Atomic Energy–Consortium for Scientific research), University Campus, Khandwa Road, Indore- 452017 (CSR-IC/ /CRS-241/2017 -18/1322).

References

[1] E.A. Neppiras, Journal of Sound and Vibration. 20 (1972) 562-563; https://doi.org/10.1016/0022-460X(72)90684-0

[2] J. Koruza, A.J. Bell, T. Frömling, K.G. Webber, K. Wang, J. Rödel, Journal of Materiomics. 4 (2018) 13-26; https://doi.org/10.1016/j.jmat.2018.02.001

[3] J. Zhao, H. Du, S. Qu, J. Wang, H. Zhang, Y. Yang, Z. Xu, Journal of Alloys and Compounds. 509 (2011) 3537-3540; https://doi.org/10.1016/j.jallcom.2010.07.153

[4] L.-Q. Cheng, M. Feng, Y. Sun, Z. Zhou, Z. Xu, J Adv Ceram. 9 (2020) 27-34; https://doi.org/10.1007/s40145-019-0344-2

[5] J. Wu, Journal of Applied Physics. 127 (2020) 190901; https://doi.org/10.1063/5.0006261

[6] N. Lartcumfu, C. Kruea-In, N. Tawichai, G. Rujijanagul, Ferroelectrics. 456 (2013) 14-20; https://doi.org/10.1080/00150193.2013.846171

[7] Y. Li, K. Moon, C.P. Wong, Science. 308 (2005) 1419-1420; https://doi.org/10.1126/science.1110168

[8] B.-P. Zhang, J.-F. Li, K. Wang, H. Zhang, J American Ceramic Society. 89 (2006) 1605-1609; https://doi.org/10.1111/j.1551-2916.2006.00960.x

[9] P.K. Panda, B. Sahoo, Ferroelectrics. 474 (2015) 128-143; https://doi.org/10.1080/00150193.2015.997146

[10] B.R. Powell, Jr, Office of Scientific and Technical Information (OSTI), 1971; https://doi.org/10.2172/4701954

[11] H. Jaffe, J American Ceramic Society. 41 (1958) 494-498; https://doi.org/10.1111/j.1151-2916.1958.tb12903.x

[12] T.R. Shrout, S. Zhang, J Electroceram. 19 (2007) 185-185; https://doi.org/10.1007/s10832-007-9095-5

[13] Y.-M. Li, Z.-Y. Shen, F. Wu, T.-Z. Pan, Z.-M. Wang, Z.-G. Xiao, J Mater Sci: Mater Electron. 25 (2013) 1028-1032; https://doi.org/10.1007/s10854-013-1682-4

[14] E.D. Politova, N.V. Golubko, G.M. Kaleva, A.V. Mosunov, N.V. Sadovskaya, S.Yu. Stefanovich, D.A. Kiselev, A.M. Kislyuk, P.K. Panda, J. Adv. Dielect. 08 (2018) 1850004; https://doi.org/10.1142/S2010135X18500042

[15] J. Rödel, W. Jo, K.T.P. Seifert, E.-M. Anton, T. Granzow, D. Damjanovic, Journal of the American Ceramic Society. 92 (2009) 1153-1177; https://doi.org/10.1111/j.1551-2916.2009.03061.x

[16] L. Luo, C. Chen, H. Luo, Y. Zhang, K. Zhou, D. Zhang, CrystEngComm. 17 (2015) 8710-8719; https://doi.org/10.1039/C5CE01382H

[17] S. Park, A. Rahman, Y. Min, G.-T. Hwang, J.-J. Choi, B.-D. Hahn, K.-H. Cho, J. Woo Lee, S. Nahm, C.-W. Ahn, Journal of the European Ceramic Society. 40 (2020) 1232-1235; https://doi.org/10.1016/j.jeurceramsoc.2019.11.007

[18] D.S. Chakram, V.R. Reddy, S.N. Kumar, M. Dasari, Journal of Inorganic and Organometallic Polymers and Materials. Springer Science and Business Media LLC (2023); https://doi.org/10.1007/s10904-023-02710-z

[19] B. Timmer, W. Olthuis, A. Van Den Berg, Sensors and Actuators B: Chemical, 107(2), 666-677; https://doi.org/10.1016/j.snb.2004.11.054

[20] M. A Sutton, J. W.Erisman, F. Dentener, D. Möller. (2008), Environmental Pollution, 156(3), 583-604; https://doi.org/10.1016/j.envpol.2008.03.013

[21] D.Kwak, Y. Lei, R. Maric. (2019), Talanta, 204, 713-730; https://doi.org/10.1016/j.talanta.2019.06.034

[22] K. Radhi Devi, G. Selvan, M. Karunakaran, I.L. Poul Raj, V. Ganesh, S. AlFaify, Materials Science in Semiconductor Processing. 119 (2020) 105117; https://doi.org/10.1016/j.mssp.2020.105117

[23] Y. Vijayakumar, P. Nagaraju, V. Yaragani, S.R. Parne, N.S. Awwad, M.V. Ramana Reddy, Physica B: Condensed Matter. 581 (2020) 411976; https://doi.org/10.1016/j.physb.2019.411976

[24] G.K. Mani, J.B.B. Rayappan, Journal of Alloys and Compounds. 582 (2014) 414-419; https://doi.org/10.1016/j.jallcom.2013.07.146

[25] U. Godavarti, V.D. Mote, M.V.R. Reddy, P. Nagaraju, Y.V. Kumar, K.T. Dasari, M.P. Dasari, Physica B: Condensed Matter. 553 (2019) 151-160; https://doi.org/10.1016/j.physb.2018.10.034

[26] U. Godavarti, V.D. Mote, M. Dasari, Electronic Materials. 3 (2017) 179-185; https://doi.org/10.1016/j.moem.2017.10.006

[27] A.A. Parfenov, O.R. Yamilova, L.G. Gutsev, D.K. Sagdullina, A.V. Novikov, B.R. Ramachandran, K.J. Stevenson, S.M. Aldoshin, P.A. Troshin, J. Mater. Chem. C. 9 (2021) 2561-2568; https://doi.org/10.1039/D0TC03559A

[28] C. Wang, X. Cui, J. Liu, X. Zhou, X. Cheng, P. Sun, X. Hu, X. Li, J. Zheng, G. Lu, ACS Sens. 1 (2015) 131-136; https://doi.org/10.1021/acssensors.5b00123